Electronic Materials Letters, Vol. 1, No. 2 (2005), pp. 135-139

Polystyrene Nanosphere Lithography Improved by the Insertion of a Sacrificial Polyimide Film

Nu Ri Oh, Tae Jin Song, Sung Keun Lim, and Chong Seung Yoon*

Department of Advanced Materials Science, Hanyang University, Seoul 133-791, Korea

A 2-dimensional hexagonal array of uniformly sized nano-holes, whose average size can be potentially changed from 50 nm to 240 nm, was fabricated using the etched nanosphere lithography (NSL) method. The conventional NSL method utilizing polystyrene beads (PS) coated on a Si substrate often suffers from a loss of uniformity during the etching of the PS beads. It was demonstrated that the uniformity of the hole size and position can be greatly improved by inserting a polyimide (PI) film between the Si substrate and the PS beads. A sufficiently thick (~40 nm) PI film can act as a sacrificial layer, minimizing the rebound of the plasma during the reactive ion etching of the PS beads. Hence, the etching of the PS beads stabilized by the PI film can be used to determine the final desired size of the hole. The periodicity of the pattern can also be selected by changing the initial PS bead diameter.

Keywords: nanopattern, polystyrene, nanosphere lithography, polyimide

1. INTRODUCTION

The recent impetus for research in nanotechnology partly stems from the fact that this new technology will provide opportunities for scientists and engineers to produce material systems with new physical and chemical properties, widely different from their non-nano-sized counterparts, by reducing their size to the nanometer scale. Possible applications for the nanostructured materials range over many areas: high density magnetic storage media[1,2], wave guides[3], biosensors[4], low dimensional electronic systems[5] and templates for nanotube growth[6, 7].

The most typical fabrication process for the patterned array of a nanostructure is photolithography[8], which is an integral part of conventional semiconductor technology. It is suitable for mass production, but currently has a resolution limit of 0.1 μm. For a very high resolution, electron beam lithography (EBL) can improve the resolution to 5 nm[9-10]; however, an EBL-patterned area is unlikely to exceed 1 mm^2 due to low throughput. Moreover, EBL also demands a great expense which makes it unsuitable for general applications. Another fabrication process is the self-assembled system[11-14]. Although this system is relatively simple and inexpensive, it also has drawbacks. Inherent in self-assembled systems is a difficulty in the precise control of the self-assembled structure, and a lack of robustness for industrial applications. With this in mind, however, the nanosphere lithography (NSL) method[15-16], which uses a self-assembled template of polystyrene (PS) or silica beads, offers a new opportunity to improve the controllability of a self-assembled system, with a low cost. It can be a valuable tool for producing prototype nano-patterned samples.

A regularly arranged nanostructure can be fabricated from an etched NSL in which the PS beads are etched to a desired size after self-assembling, so that the masked area can be altered by adjusting the etching time. In this paper, we present an improvement over previous etched NSL processes. Our experimental process consists of inserting a thin film of polyimide between the substrate and the PS beads to provide a better anchoring of the PS beads during the etching process, thus improving the uniformity in size, and the position of the patterns.

2. EXPERIMENTAL PROCEDURE

The fabrication procedure is schematically described in Fig. 1. A polyimide (PI) precursor (polyamic acid (PAA)) solution was spin coated onto a Si wafer. The PAA used in this experiment was a *p*-phenylene biphenyltetracarboximide (BPDA-PDA) type polyamic acid (Dupont, PI2610D) dissolved in *N*-Methyl-2Pyrrolidinone. The thickness of the spin-coated PI precursor was controlled so that the final cured thickness of the PI layer varied from 1.7 nm to 40 nm when heat treated at 400 ^{o}C in a vacuum (10^{-3} Pa)[17]. Monodisperse PS beads with a diameter of 260 nm (Bangs Labo-

*Corresponding author: csyoon@hanyang.ac.kr

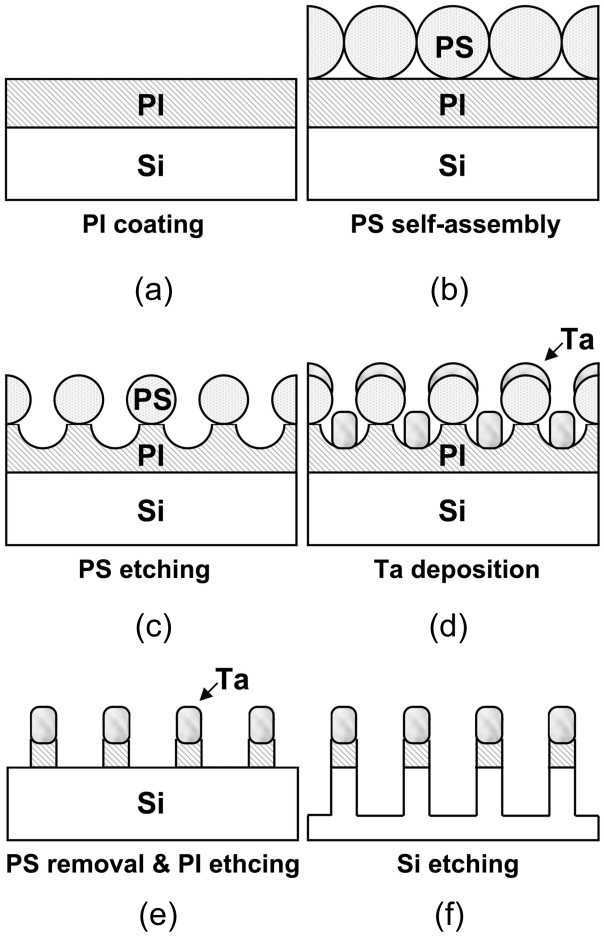

Fig. 1. Schematic diagram of the fabrication process. (a) Coating of the PI film on a Si substrate, (b) self-assembly of the PS beads, (c) reduction of the PS bead diameter using RIE, (d) Ta deposition by DC magnetron sputtering, (e) removal of the PS beads and etching of the patterned PI using RIE, (f) formation of the nano-hole array using RIE.

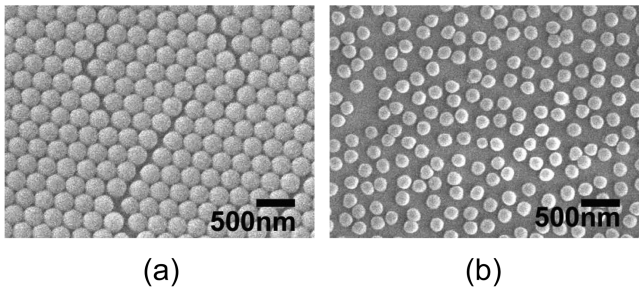

Fig. 2. SEM images of the PS beads from Si/PS samples. (a) prior to RIE, (b) after 5 min of RIE.

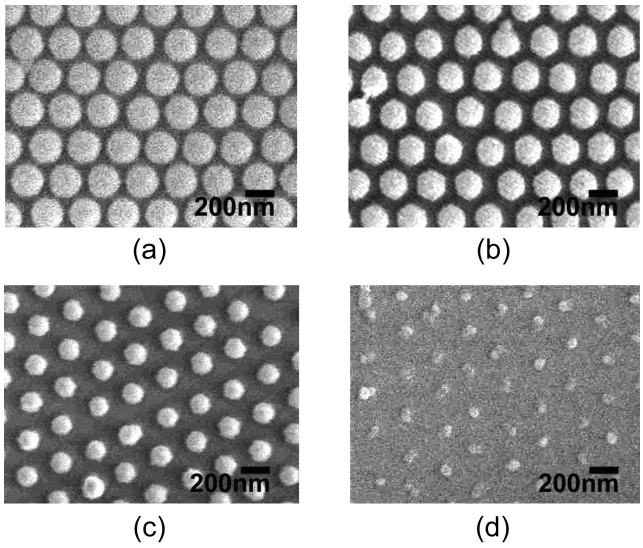

Fig. 3. SEM images of the etched PS beads from Si/PI (40 nm)/PS samples: (a) for 5 min, (b) for 7 min, (c) for 9 min and (d) for 13 min.

ratories, USA) were dispersed in a solution containing a surfactant, Triton X-100 (Aldrich), and methanol (diluted to 1:400 by volume) by a factor of 1.0[18] in order to wet the substrate. The PS solution was then spin coated onto the PI layer (~2 cm^2 in area) at 1000-2000 rpm. The PS beads were then thinned by reactive ion etching (RIE) in an argon-oxygen atmosphere in a chamber pressure at 100 mTorr and a gas flow rate of 15 sccm for both gases.

After the RIE, a 40-nm-thick layer of Ta was deposited on the sample as an etching mask layer using a magnetron sputtering system. Following this, the PS beads were removed from the PI layer in an ultrasonic bath of toluene, leaving behind the patterned PI film. The protruding PI region, not covered by the Ta film, was etched by RIE for 10 min under the abovementioned conditions. The exposed part of the Si substrate was etched again by RIE with a mixture of carbon fluoride and oxygen (CF_4 : O_2 = 10 : 1) at 150 W and 55 mTorr for 120 sec. Since Ta has a higher etching resistance than does Si, an array of nano-holes was formed. Scanning electron microscopy (SEM, JSM 6330F) and transmission electron microscopy (TEM, JEOL 2010) were used to characterize the self-assembled polystyrene beads and nano-patterns.

3. RESULTS AND DISCUSSION

Figure 2(a) shows a SEM image of a self-assembled mono-layer of PS spheres coated on the Si substrate without the PI layer. When the PS beads were etched for 3 min, the average diameter of the individual PS beads was reduced from 260 nm to 220 nm while maintaining the original hexagonal lattice. However, as shown in Fig. 2(b), etching for 5 min not only reduced the average bead diameter to 195 nm but also led to a loss of uniformity in the PS lattice. Haginoya et al. have suggested that such non-uniformity can arise from the distribution in the size and shape of the initial PS beads, non-uniform O_2 RIE rate and defects in the PS bead

Table 1. Mean particle diameter and standard deviation of the etched PS beads from the samples: Si/PS and Si/PI (40 nm)/PS.

		Etching Time (min)					
Sample		3	5	7	9	11	
Si/PS	Mean size (nm)	219.3	194.9	87.05			
	Stand. Dev. (nm)	7.2	9.5	11.9			
Si/PI	Mean size (nm)	239.2	230.7	200	160.3	96	70.6
(40 nm)/PS	Stand. Dev. (nm)	3.3	4.2	3.8	7.2	15.1	20.0

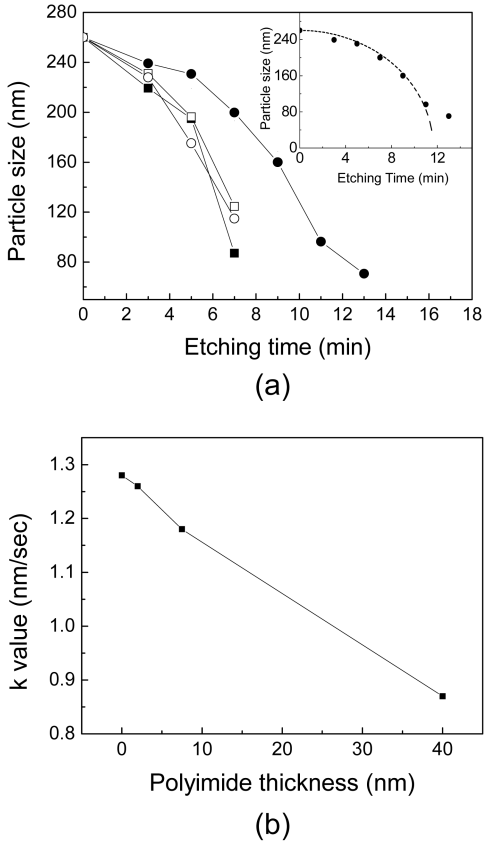

Fig. 4. Relationship between: (a) the etching time and PS diameter at different PI thicknesses, (b) k value in Haginoya's equation and the polyimide thickness. (■: Si/PS, ●: Si/PI(40 nm)/PS, □: Si/PI(7.5 nm)/PS, ○: Si/PI(1.5 nm)/PS) The inset in (a) shows the PS diameter at different etching time (solid dot), obeying Haginoya's empirical expression with k=0.87 (dotted line).

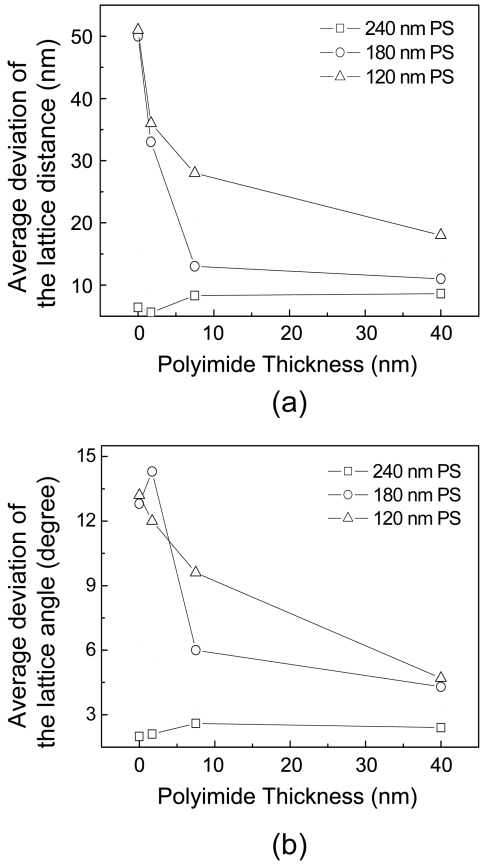

Fig. 5. (a) deviation of the nearest neighbor distance of 260 nm in the hexagonal lattice and (b) angular deviation from 60° of the nearest neighbor interparticle angles at different PI film thicknesses.

lattice[15]. Compared to the etched PS array on the Si substrate shown in Fig. 2(b), when a 40-nm-thick PI film was inserted between the Si substrate and the PS beads, the PS bead lattice was well maintained even at an extended etching period, as can be seen Fig. 3(a)-(d). Table 1 compares the mean PS bead diameter after different etching periods. Table 1 clearly shows that the mean PS diameter was much larger with the PI layer than without, which indicates that the insertion of the PI film decreased the RIE rate, and that the PI film acted as a sacrificial layer. Although the 7-min etching made a PS bead size similar to that of the 5-min etching without the PI layer, the standard deviation of the bead diameter without the PI underlayer was considerably larger than that of the sample which had a 40-nm-thick PI layer under the PS beads. It appears that the PI sacrificial layer not only helps to maintain the lattice structure, but also decelerates the overall etching rate of the PS beads while reducing the variation in the etching rate.

To further probe the effect of the PI layer, a PI film with two other thicknesses (1.5 nm and 7.5 nm) was inserted between the Si substrate and the PS beads. Fig. 4 (a), which plots the average PS diameter as a function of etching time for different PI thicknesses indicates that increasing the PI film thickness tends to lower the RIE rate, but the effect is

hardly noticeable for the 1.5- and 7.5-nm-thick PI films. In all cases, however, the etched bead diameter was well matched with Haginoya's empirical expression [15] which relates the etching time, t with the sphere diameter, d:

$$d = d_0 \cos[\arcsin(kt / 2d_0)] \quad (1)$$

where d_0 is the initial diameter of PS, and k is a constant depending on the etching conditions. The inset in Fig. 4(a) clearly shows the experimental data (solid dot) from the SI/PI (40 nm)/PS sample obeying Haginoya's equation with k = 8.7, although the bead diameter began to deviate from eq. (1) when the etched PS diameter was below 80 nm. Furthermore, estimated k *values* exhibited an approximate linear dependence on the PI thickness, as shown in Fig. 4(b). However, it is expected that the k value will eventually plateau when the PI film became excessively thick.

In Fig. 5, we quantitatively studied the ordering of the PS beads when the PI film was inserted by estimating the deviation of the nearest-neighbor distance and interparticle angle from a perfect hexagonal lattice. The PS beads were etched until the mean diameter reached 240 nm, 180 nm, and 120 nm by varying the etching time. The average deviations from 260 nm and 60° were estimated from the SEM micrographs and plotted in Fig. 5(a) and (b). Fig 5(a) and (b) show that the effect of the PI underlayer was minimal when the average PS bead diameter was 240 nm, but became increasingly noticeable as the bead size was reduced by etching. Fig. 5 clearly demonstrates that the presence of the PI underlayer helps to maintain the ordered structure by providing a better anchoring. From the fact that the thick PI film was more effective in retaining the lattice structure, it is inferred that the PI layer acted as a sacrificial layer during the etching of the PS beads.

Si substrate should be etched only slightly by the oxygen-argon plasma under the given conditions. It is surmised that the plasma which goes through the voids among the PS beads impinges on the Si surface and is subsequently rebounded toward the bottom area of the PS beads. This rebound causes a rapid etching of the PS beads, breaking away the PS beads from the Si substrate. When the PI film is inserted, however, the plasma etches the PI underlayer instead, minimizing this rebound effect. SEM and cross-sectional TEM images of the PI layer after removing the etched PS beads in Fig. 6(a) revealed that the PI underlayer directly underneath the PS beads remained intact (arrowed in the TEM image in the inset), while the area around the PS beads was etched to 20 nm thick after 7 minutes of etching. When the etching time was extended to 11 min, the PI layer was completely removed by the plasma except at the original positions where the PS beads had existed, as can be seen from Fig. 6(b). This clearly shows that the PI underlayer was preferentially etched. The PI underlayer slows down the etching rate of the PS beads, and acts as a sacrificial layer while providing an anchoring support for the beads during RIE.

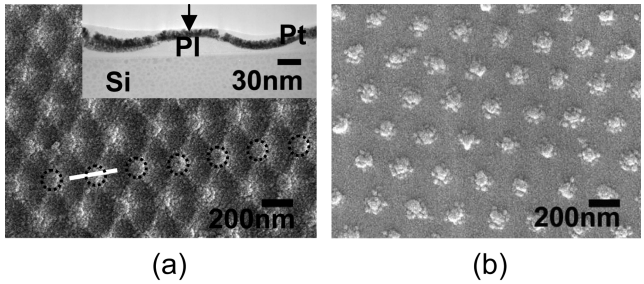

Fig. 6. SEM images of the patterned nano-holes after removal of the PS beads that were etched for (a) 7 min and (b) 11 min. (Circles in (a) indicate the original PS positions.) The inset image in (a) is a cross-sectional TEM image of the region shown by a white line in (a), and Pt was coated to provide a better contrast between the epoxy and the polyimide.

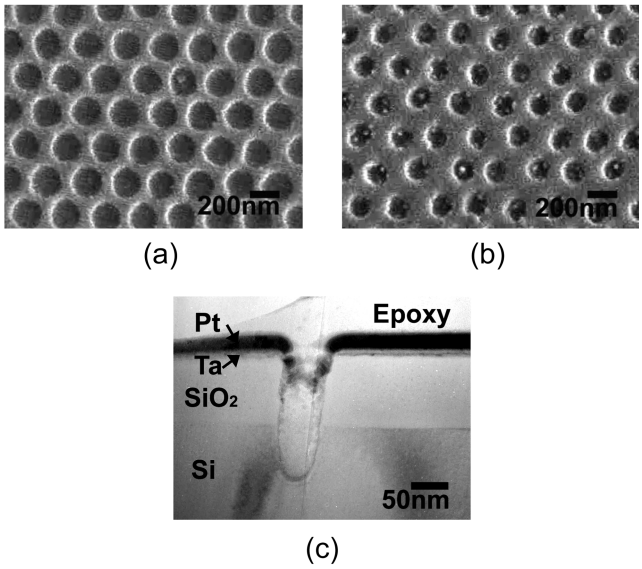

Fig. 7. SEM images of nano-patterns after etching the Si substrate for 250 sec: from the Si/PI (40 nm)/PS sample with the PS beads etched for (a) 7 min, and (b) 9 min, (c) TEM cross-sectional image of the 50-nm-sized hole pattern from Si/SiO_2/PI (40 nm)/PS sample with the PS beads etched for 13 min. Pt was coated to provide a better contrast.

After etching the PS beads to a desired size, the Si substrate was further processed, as described in Fig. 1. The positions where the PS beads had previously been located were preferentially etched while the rest of the area was masked by the Ta film and generated regularly spaced nano-holes. The nano-holes have the regular sizes and positions retained from the PS beads, as can be seen from the holes made from the Si/PI(40nm)/PS sample in Fig. 7(a) and (b). Nanopatterns in Fig. 7(a) and (b), whose respective hole diameters were 180nm and 130 nm, were fabricated from the 200-nm- and 160-nm-sized PS beads while the periodicity of the holes was maintained at 260 nm, as determined by the initial diameter of the PS bead prior to etching. The reason for the

reduced hole size compared to the bead diameter is likely due to the fact that the Ta film was not completely shadowed by the PS beads, but instead was partially deposited under the PS beads. Figure 7(c) shows a cross-sectional TEM image of a hole whose diameter is 50 nm. This was made from the 13 min-etched Si/SiO_2/PI (40 nm)/PS sample. The Pt film was deposited to enhance the contrast. The diameter of the hole was well maintained throughout the depth of the hole. It should be noted that the material inside the hole in Fig. 7(c) is from the Pt film, not from the Ta mask.

4. CONCLUSION

We demonstrated that an array of uniformly sized nanoholes can be fabricated by the etched NSL method when a PI sacrificial layer is inserted between the substrate and the PS beads. The hole size can be easily controlled by adjusting the etching time. Moreover, the periodicity of the hole pattern can also be changed by use of the initial PS beads with a different size. Such patterned holes can be filled with magnetic or electroluminescent materials to produce functional nanostructures. It is expected that the method will have a wide rage of applications in nano-science and technology.

ACKNOWLEDGEMENT

This work was supported by the Ministry of Science and Technology through the Nanoscopia Center of Excellence at Hanyang University.

REFERENCES

1. N. Singh, S. Goolaup, and A. O. Adeyeye, *4th IEEE conference on nanotechnology,* p. 65, Munich, Germany (2004).
2. T. Sannomiya, J. Shi, Y. Nakamura, and O. Nitto, *J. Appl. Phys*. **96**, 5050 (2004).
3. S. A. Maier, P. G. Kik, H. A. Atwater, S. Meltzer, E. Harel, B. E. Koel, and A. A. G. Requicha, *Nat. Mater.* **2**, 229 (2003).
4. X. Ren, X. Meng, D. Chen, F. Tang, and J. Jia, *Biosens. Bioelectron*. **21**, 433 (2005).
5. Y. Suganuma and A. Dhirani, *J. Phys. Chem. B* **109**, 15391 (2005).
6. Z. P. Huang, D. L. camahan, J. Rybczynski, M. Giersig, M. Sennett, D. Z. Wnag, J. G. Wen, K. Kempa, and Z. F. Ren, *Appl. Phys. Lett.* **82**, 460 (2003).
7. J. Wang, M. Zhu, X. Zhao, R. A. Outlaw, D. M. Manos, B. C. Holloway, C. H. Park, T. Anderson, and V. P. Mammana, *J. Vac. Sci. Technol. B* **22**, 1268 (2004).
8. L. R. Harriott and R. Hull, *Introduction to nanoscale science and technology, 1st ed.* (eds., M. D. Ventra, S. Evoy and J. R. Jr. Heflin), p. 7, Kluwer Acedimic Publishers, Norwell, Mass (2004).
9. B. Cui, W. Wu, L. S. Kong, X. Y. Sung, and S. Y. Chou, *J. Appl. Phys.* **85**, 5534 (1999).
10. T. Ito and S. Okazaki, *Nature* **406**, 1027 (2000).
11. J. Y. Cheng, A. M. Mayes, and C. A. Ross, *Nat. Mate.* **3**, 823 (2003).
12. C. L. Haynes and R. P. Van Duyne, *J. Phys, Chem. B* **105**, 5599 (2001).
13. W. J. Yu, Y. S. Cho, G. S. Choi, and D. J. Kim, *Nanotechnology* **16**, S291 (2005).
14. G. Zhang, D. Wang, Z. Gu, J. Hartmann, and H. Moehwald, *Chem. Mater.* **17**, 6268 (2005).
15. C. Haginoya, M. Ishibashi, and D. Koike, *Appl. Phys. Lett.* **20**, 2934 (1997).
16. S. M. Weekes, F. Y. Ogrin, and W. A. Murray, *Langmuir* **20**, 11208 (2004).
17. S. K. Lim, C. S. Yoon, C. K. Kim, and Y. H. Kim, *J. Phys. Chem*, *B* **108**, 18179 (2004).
18. J. C. Hulteen, D. A. Treichel, M. T. Smith, M. L. Duval, T. R. Jensen, and R. P. Van Duyne, *J. Phys. Chem. B* **103**, 3804 (1999).